

Third sound and energetics in ^3He - ^4He mixture films

P. A. Sheldon and R. B. Hallock

Laboratory for Low Temperature Physics, Department of Physics and Astronomy, University of Massachusetts at Amherst, Amherst, Massachusetts 01003

(Received 16 May 1994)

We report measurements of the third-sound frequency and attenuation in a capacitive resonator as a function of temperature for various submonolayer densities of ^3He ($0.007 \leq n_3 \leq 0.049 \text{ \AA}^{-2}$) in a thin ^4He film ($n_4 = 0.389 \text{ \AA}^{-2}$), which result in a determination of the ground-state and first-excited-state energies for the ^3He which are in good agreement with the energetics determined by NMR. Interesting features are seen in the temperature dependence of the frequency and phase of the third sound for $100 < T < 200$ mK.

Helium mixture films bound to a substrate are rich with information about the quasi-two-dimensional properties of Fermi systems. In a ^4He film ^3He occupies bound states perpendicular to and free-particle states parallel to the substrate.¹ In its lowest energy state, a ^3He atom resides at the surface of the ^4He film. The ^3He has higher energy states available to it, ϵ_i , which are apparently located inside the ^4He film. Bhattacharyya, Di Pirro, and Gasparini² measured the bound-state energies of ^3He on a ^4He film using heat-capacity techniques. More recently the ground-state energy, ϵ_0 , and the energy difference between the ground state and first excited state, Δ , has been measured^{3,4} using NMR for a large range of ^4He film thicknesses with a fixed coverage of ^3He , and for many submonolayer coverages of ^3He on a fixed thickness of ^4He .⁵ We report here measurements of the temperature and ^3He density dependence of the frequency, damping and phase of third-sound resonance modes. The energetics of the ^3He Fermi system are extracted from the data and compared to our results for the energetics determined⁵ by NMR techniques. We document unexplained behavior: a weak but persistent maximum in the third-sound frequency near 150 mK and a dramatic temperature dependence of the phase for $150 < T < 200$ mK.

Third sound⁶ is a temperature and areal density wave which propagates on superfluid helium films. Such films can exist on most solid surfaces due to the van der Waals attractive interaction between the helium atoms and the atoms of the solid substrate. The third-sound velocity for a pure ^4He film is given by the approximate expression⁷

$$C_{30}^2 \approx \rho_s / \rho (1 - D/d_4) \vartheta d_4 [1 + TS/L]^2,$$

where ρ_s / ρ is the bulk superfluid fraction, D is the thickness of the immobile part of the film adjacent to the substrate, d_4 is the thickness of the film, and ϑ , S , L are the van der Waals force, entropy, and latent heat per unit mass. Over the temperature range of this work, $TS/L \approx 0$, $\rho_s / \rho \approx 1$, D is constant,⁸ and ϑ varies only with ^4He film thickness.

The third-sound frequency (f), quality factor (Q), amplitude (A) and phase between the drive and detected amplitude (Φ) are measured with a third-sound resonator which is mounted in a copper cell alongside an NMR coil. The cell is attached to a dilution refrigerator. The

third-sound resonator is constructed from a rectangular piece of Nuclepore, 14.3×19.1 mm. The Nuclepore is $10 \mu\text{m}$ thick, with $\sim 3 \times 10^8$ pores/cm², and each pore has a 2000 \AA diameter. 90% of the surface area is inside the pores. A silver strip is evaporated onto one end of the resonator to drive the third sound thermally, and capacitor plates are evaporated onto both sides at the opposite end to detect thickness changes capacitively. The capacitor is part of an LC tank circuit driven by a tunnel diode oscillator which oscillates at a nominal frequency of 25 MHz. When the third-sound modes are driven (~ 300 Hz) the film thickness between the capacitor plates changes sinusoidally. The resulting frequency modulation is detected with a phase lock loop, and the amplitude of a driven frequency is measured by lock-in detection with the drive frequency as reference. The sensitivity of the frequency of the LC circuit to film thickness is measured as 30 Hz/\AA ; we are able to measure third-sound film thickness changes of $2.5 \mu\text{ \AA}$. f , A , Q , and Φ for a third-sound mode are measured by sweeping the drive through the resonant frequency, and performing a four-parameter fit of the in-phase and quadrature amplitudes versus frequency to a Lorentzian. All data reported here are for the fundamental mode f_1 .

We vary the amount of ^3He in a film of ^4He , $n_4 = 0.389 \text{ \AA}^{-2}$ ($d_4 = 3.65$ layers). For each of the eight ^3He densities in the range $0.007 \leq n_3 \leq 0.049 \text{ \AA}^{-2}$ ($0.099 \leq d_3 \leq 0.721$ layers) described here, we made measurements in the temperature range $40 \leq T \leq 500$ mK for drive powers $0.044 \leq P_{\text{dr}} \leq 440$ nW. As expected, the amplitude goes to zero at zero drive power, and it rises linearly with drive power for small P_{dr} .⁹ The frequency is observed to be a linear function of drive power, and can be extrapolated back to zero drive power with negligible error. The Q is independent of drive at the lower drive powers, except apparently at the very lowest drive powers where it is also quite imprecise. Unless otherwise specified, the frequency reported here is extrapolated to $P_{\text{dr}} = 0$. The Q 's at the lowest three drive powers are extrapolated to obtain the $P_{\text{dr}} \rightarrow 0$ limit.

A simple quantitative description for the third-sound velocity in a mixture film system of ^3He and ^4He can be derived from a set of linearized hydrodynamic equations^{10,11} by assuming that there are two layers; the lower

layer (l) contains all the superfluid and some concentration of ^3He and the upper layer (u) is a normal fluid blanket of ^3He . The theory assumes that the helium is incompressible and that there are no interaction effects between the two layers. The result for the third-sound velocity in a mixture film at $T=0$ is

$$C_3^2 = C_{30}^2 \left(\frac{m_4}{m_l} \right) \left(\frac{d_4}{d_l} \right)^4 \left[1 - \frac{\rho_u}{\rho_l} + \frac{\rho_u/\rho_l}{(1+d_u/d_l)^4} \right], \quad (1)$$

where C_{30} is the third-sound velocity for a film of pure ^4He of thickness d_4 , and d_4 is the thickness of the film if there were no ^3He , m_4 is the mass of a ^4He atom, m_l is the average mass per particle in the lower layer, ρ_u and ρ_l are the average number densities in the upper and lower layers, and d_u and d_l are the thicknesses of those layers. We can add temperature dependence to the film thicknesses d_u, d_l in Eq. (1) by assuming that as the temperature increases, the ^3He is both excited into its higher-energy state inside the ^4He film and evaporated into the vapor. Thus the various parameters of Eq. (1) can be expressed in temperature-dependent forms which depend on the energetics of the ^3He .

In order to calculate the ^3He population densities of the bound states and the vapor, we need to know the chemical potential everywhere. The chemical potential of a dilute vapor of ^3He atoms is $\mu_v = k_B T \ln(1/2\rho_v \lambda_T^3)$, where ρ_v is the ^3He number density in vapor and $\lambda_T = \sqrt{2\pi\hbar^2/mk_B T}$ is the thermal de Broglie wavelength. Edwards *et al.*¹² propose a simple interaction term in the chemical potential of the film, $\mu_f = \epsilon_B + 1/2n_3 V_0^S + \mu_{\text{IFG}}$, where n_3 is the ^3He areal density, ϵ_B is the ^3He binding energy to the film, V_0^S is a quasiparticle interaction potential and $\mu_{\text{IFG}} = k_B T \ln[\exp(n_3 \pi \hbar^2 / m^* k_B T) - 1]$ is the chemical potential of an ideal two-dimensional Fermi gas. The effective mass m^* of a ^3He atom in a mixture film is derived at low ^3He densities using the susceptibility measurements¹³ from NMR and Fermi-liquid parameters calculated by Krotscheck, Saarela, and Epstein.^{14,15} We measure $m^* = 1.5m$, and use this value for the higher ^3He coverages since it is predicted^{15,16} to change very little over our range of densities. Bhattacharyya, DiPirro, and Gasparini² also show that there is little ^3He dependence of m^* above $n_3 \approx 0.01 \text{ \AA}^{-2}$. Equating the expressions for μ_v and μ_f , the fraction of ^3He atoms which evaporate from the film, $p_v \equiv \rho_v V/N$, where V is the volume of the sample cell, can be determined if we add the additional constraint that particle number is conserved, $N = \rho_v V + n_3 A$, where A is the area of the film.

Sprague *et al.*³ were able to solve this problem analytically by making a number of reasonable assumptions. In calculating the number of ^3He atoms in the vapor they found that they did not need to include the effects of evaporation into the first excited state because it has an energy very near to the vapor phase, and has a phase space which is smaller by a factor of $V/\lambda_T A$. At temperatures where evaporation is prevalent (above 300 mK), there is very little ^3He mixed into the lower ^4He layer, and the ^3He in the vapor will dominate the effect of any ^3He in an excited state. For our higher ^3He densities the quasipar-

ticle interaction term is small but not negligible; using the value for ^3He on bulk ^4He , $V_0^S = 11.6 \text{ K \AA}^2$,¹⁷ $\frac{1}{2}n_3 V_0^S$ is 5% of ϵ_B for our highest density. We use μ_f exactly, and still ignore the negligible effects of ^3He evaporating into higher-energy states in the film at temperatures above 300 mK. This results in a nonanalytic function for the fraction of ^3He atoms left in the film during evaporation, and that quantity can be determined numerically.

For the ^3He in the film, we need to derive the fraction of ^3He atoms in each state, $n_i A/N$, at all temperatures. For lower ^3He densities it is adequate to use a Boltzmann distribution for a two-state system so that $n_1 A/N = \exp(-\Delta/k_B T)$, where $\Delta + \epsilon_F = \epsilon_1 - \epsilon_0$. For higher densities, the film has the properties of a two-dimensional Fermi gas. We use the chemical potential for each energy state in the film, $\mu_i = \epsilon_i + \frac{1}{2}n_i V_0^S + \mu_{\text{IFG}_i}$, where ϵ_i , n_i , and μ_{IFG_i} are the energy, areal density, and ideal Fermi gas chemical potential of state i , respectively. Conserving the number of ^3He atoms, $N = \sum_i N_i$, and noting that the chemical potential is the same everywhere, we can solve for the ground- and first excited states to give a nonanalytic equation for one quantity, either $p_0 \equiv n_0 A/N$ or $p_1 \equiv n_1 A/N$, which can be solved numerically. With the numerical functions for the probability distributions p_v , p_0 , and p_1 we interpret the features seen in the third-sound data and extract values for the bound-state energies, comparing them to those found from NMR.

The temperature dependence of the third-sound frequency is shown in Fig. 1(a) for eight different ^3He densities. As seen previously,¹¹ at low temperatures the third-sound frequency has the expected dependence on ^3He thickness according to Eq. (1) for a phase-separated film (the lower layer being *nearly* all ^4He and the upper, ^3He). The film is expected to be completely phase separated at $T=0$ as determined by the energetics because the ground state of the ^3He is at the surface of the ^4He film.¹

At low temperatures ($T \leq 150$ mK) the ^3He is in its ground state at the surface of the ^4He film, and the frequency has little structure. There is a small maximum at 150 mK which gets relatively larger as ^3He density is increased. This is similar to the anomaly reported earlier.¹⁸ This peak was seen to be much more dramatic¹⁹ at considerably higher ^3He densities. The frequency decrease in the range $150 \text{ mK} \leq T \leq 300 \text{ mK}$ is attributed²⁰ to the ^3He being excited into a higher-energy state. If the higher-energy state is inside the ^4He film, then the film becomes effectively thicker, and the third-sound frequency should decrease. For the higher ^3He densities reported here, the application of Eq. (1) with the temperature dependence included in the layer thicknesses leads us to expect a more gradual decrease in frequency with increased temperature for any reasonable energy difference Δ between the first two states than is observed. For $T > 300$ mK the frequency increases due to ^3He evaporating from the film. We can fit Eq. (1) to the increasing part of the frequency vs temperature curve, with the binding energy in the probability density of the vapor as a parameter. In the region where evaporation is prevalent, as argued above, the ^3He evaporating from the top of the ^4He dominates the effect of the ^3He mixing into the ^4He

film, so we use the phase-separated form of Eq. (1),

$$\left[\frac{C_3(T)}{C_{30}(T)} \right]^2 = 1 - \frac{\rho_3}{\rho_4} \left[1 - \left(1 + \frac{d_3(T)}{d_l} \right)^{-4} \right], \quad (2)$$

where d_l is the lower layer thickness needed to account for the frequency reduction between the lowest temperature (where it is truly a layered film) and the minimum of the f vs T curve, presumably due to a small amount of ^3He mixed into the lower layer. From the fits of Eq. (2) to data, we can determine the ground-state binding energy of ^3He to the ^4He film for each ^3He density. The fits to the evaporation region are shown in Fig. 1(a) for selected ^3He densities as smooth curves.

The excess attenuation is the additional attenuation as ^3He is added to the ^4He film, $R_{\text{ex}} \equiv 1/Q - 1/Q_0$, where Q_0^{-1} is the attenuation for the lowest ^3He density, $n_3 = 0.007 \text{ \AA}^{-2}$. The excess attenuation R_{ex} is observed to be thermally activated^{20,21} with an empirical form $R_{\text{ex}} = R_0 + R_1 p_1$, where R_0 and R_1 are arbitrary parameters and p_1 is the first-excited-state probability distribution for a two-state system with activation energy Δ' .

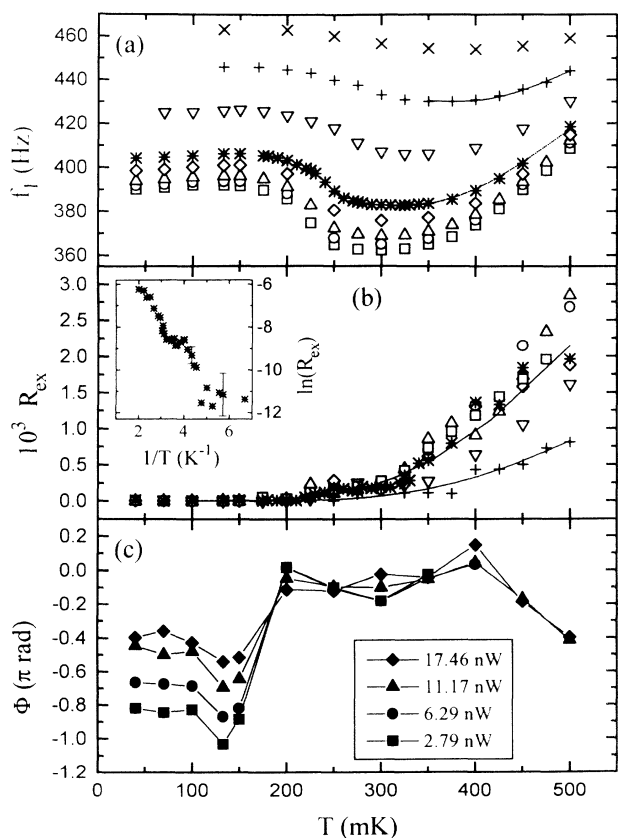


FIG. 1. Temperature dependence of (a) f_1 and (b) R_{ex} ($R_{\text{ex}} = 1/Q - 1/Q_0$, where $1/Q_0$ is the damping for the lowest ^3He coverage) for each ^3He coverage: $n_3 = 0.007$ (\times), 0.016 ($+$), 0.025 (∇), 0.036 ($*$), 0.040 (\diamond), 0.044 (\triangle), 0.046 (\circ), and 0.047 \AA^{-2} (\square). Typical fits are shown to the frequency and damping data from which the energetics are determined. The inset shows the single exponential behavior of the excess damping. (c) Phase versus temperature for a single ^3He density of 0.046 \AA^{-2} at four drive powers. Lines are drawn as a guide to the eye.

For low ^3He densities, p_1 takes the form of a Boltzmann distribution and for higher ^3He densities we use the Fermi distribution discussed earlier. By fitting the appropriate form of R_{ex} to the excess attenuation data, we can extract an activation energy, Δ' for each ^3He density. We show in the inset of Fig. 1(b) a plot of $\ln(R_{\text{ex}})$ vs $1/T$ for a ^3He density of 0.036 \AA^{-2} . Although we might expect to see multiple exponential behavior since the ^3He is first excited into a higher-energy state in the film and then at higher temperatures is evaporated into the vapor, the data show only a single exponential. This indicates that the excess damping is more sensitive to the ^3He inside the ^4He film rather than the ^3He on top, as might be expected since the ^3He in the ^4He contributes to the normal component. The independence of the damping from evaporation into the vapor is also evident from the fact that at low temperatures the damping does not have any apparent dependence on ^3He density. For this reason we fit the single-exponential function for R_{ex} over the entire temperature range for all the ^3He densities. The excess damping data and typical fits are shown in Fig. 1(b).

An additional property of interest available from the third-sound measurements is the phase between the drive pulse and the ^4He film thickness above the driver. It is predicted by Bergman⁷ that there should be a 180° phase difference between the temperature and the ^4He film thickness for third sound in pure ^4He films. This indicates that when the temperature of the driver is a maximum, the film thickness above it is a minimum. The quantitative relationship between temperature and film thickness oscillation predicted by Bergman was earlier measured²² for third sound in a pure ^4He film. For the current measurement on mixture films, we see that within experimental error, for all the ^3He densities, at the lowest drive powers and below 200 mK there is indeed a 180° phase difference [one ^3He coverage is shown in Fig. 1(c)]. Then, abruptly near 200 mK, the phase changes to zero, indicating that the drive and response are in phase. Below 200 mK, the higher the drive power, the closer the drive and response are to being in phase. Above 200 mK there is no drive power dependence. This general behavior may be related to the curious pulse inversion seen in earlier third-sound work at much higher coverages.²²

From the fits to the frequency data in Fig. 1 we derive the ground-state binding energy ϵ_0 , and from the fits to the excess damping data we derive an activation energy Δ' . Along with the Fermi energies from NMR measurements, we can derive an excited-state energy ϵ_1 if we assume the activation energy Δ' to be related to Δ as $\Delta' = \Delta$. These two energies are compared in Fig. 2 to the ground-state and first-excited-state energies derived from NMR.⁵ The agreement is good, which indicates that the assumption that we can ignore the higher-energy state in the film in the evaporation region is reasonable.

Also included in Fig. 2 is the theory of Anderson and Miller²³ for the ^3He density dependence of two energy states on a similar ^4He film ($d_4 = 3.4$ layers). They allowed for two states to be available in the film. We see reasonable agreement with their first excited state, especially at the higher densities, but poor agreement with the

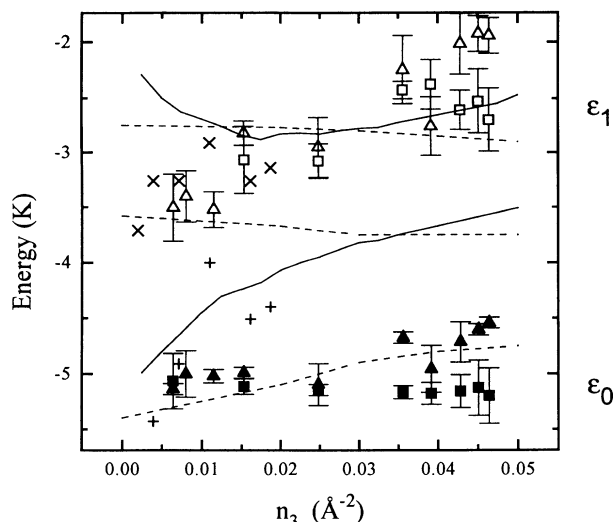


FIG. 2. Ground-state (solid symbols) and first-excited-state (open symbols) dependence on ${}^3\text{He}$ density of the binding energies of ${}^3\text{He}$ to a thin ${}^4\text{He}$ film. Energies from third sound (squares) are compared to the energies from NMR (triangles). Solid lines are theory of Anderson and Miller for a similar film. Dashed lines are theory of Pavloff and Treiner for ${}^3\text{He}$ on bulk ${}^4\text{He}$. Crosses and pluses are data from Ref. 2 for a similar film.

ground state. Pavloff and Treiner²⁴ calculate the ${}^3\text{He}$ density dependence of the surface states on bulk ${}^4\text{He}$ using a density-functional approach; the lowest three of these are included in Fig. 2. Our ground-state energies are closer to those predicted by Pavloff and Treiner for ${}^3\text{He}$ on bulk ${}^4\text{He}$ than to those predicted by Anderson and Miller. For our ${}^4\text{He}$ coverage, which is slightly higher than Anderson and Miller's, we would expect to be closer to the binding energy of ${}^3\text{He}$ on bulk ${}^4\text{He}$, but we also would expect that the binding energies *increase* towards this value as ${}^4\text{He}$ coverage is increased.³ We are also in excellent agreement with a calculation of Pavloff

and Treiner for a ${}^3\text{He}$ impurity on a ${}^4\text{He}$ film at our lowest ${}^3\text{He}$ coverage.³ In this theory they take into account the proper ${}^4\text{He}$ density profile, and allow multiple states. They also note¹ that if, instead of bulk ${}^4\text{He}$ they have a film of ${}^4\text{He}$ their highest energy shown in Fig. 2 would be "pushed up" somewhat. It is possible that in our analysis we cannot distinguish between the higher two states, and are seeing an averaging of the two. Also included in Fig. 2 are the energies from the heat-capacity data of Bhattacharyya, DiPirro, and Gasparini² for similar film configuration ($d_4 = 3.4$ layers) on Nuclepore for some low ${}^3\text{He}$ densities; agreement is reasonable for both energy states.

In summary, we have observed the progression of the third-sound frequency, damping and phase as a function of temperature and ${}^3\text{He}$ density on a thin ${}^4\text{He}$ film. From the third sound, we have derived the absolute values of the ground- and first-excited bound state energies of the ${}^3\text{He}$ to the thin ${}^4\text{He}$ film as a function of increasing ${}^3\text{He}$ density, and observe that the agreement with measurements from NMR is good. The first-excited-state energy derived from third sound is in reasonable agreement with theory, although the ground state differs somewhat. There is an interesting feature observed in the phase of the third-sound mode—the relationship between the temperature fluctuations and crest height of the third-sound wave has an abrupt 180° phase change near the temperature where the ${}^3\text{He}$ starts to evaporate into a higher-energy state.

We would like to thank J. Valles and B. R. Johnson for early help with the apparatus and D. Sprague and J. Vithayathil for their help in data taking and for useful comments. We acknowledge conversations with J. Treiner which were facilitated by a NATO travel grant. R.B.H. acknowledges the support of the J. S. Guggenheim Foundation. This work was supported by the National Science Foundation through DMR 91-22348.

¹N. Pavloff and J. Treiner, *Physica B* **169**, 537 (1991), and references therein.

²B. K. Bhattacharyya, M. J. DiPirro, and F. M. Gasparini, *Phys. Rev. B* **30**, 5029 (1984).

³D. T. Sprague, N. Alikacem, P. A. Sheldon, and R. B. Hallock, *Phys. Rev. Lett.* **72**, 384 (1994).

⁴N. Alikacem, D. T. Sprague, and R. B. Hallock, *Phys. Rev. Lett.* **67**, 2501 (1991).

⁵D. T. Sprague, N. Alikacem, P. A. Sheldon, and R. B. Hallock, *Physica B* **194-196**, 629 (1994); Ref. 3; (unpublished).

⁶K. R. Atkins, *Phys. Rev.* **113**, 962 (1959).

⁷D. J. Bergman, *Phys. Rev. A* **3**, 2058 (1971).

⁸J. H. Scholtz, E. O. McLean, and I. Rudnick, *Phys. Rev. Lett.* **32**, 147 (1974).

⁹K. S. Ketola, S. Wang, and R. B. Hallock, *Physica B* **194-196**, 649 (1994).

¹⁰R. A. Guyer and M. D. Miller, *Phys. Rev. Lett.* **47**, 349 (1981).

¹¹F. M. Ellis, R. B. Hallock, M. D. Miller, and R. A. Guyer, *Phys. Rev. Lett.* **46**, 1461 (1981).

¹²D. O. Edwards, S. Y. Shen, J. R. Eckardt, P. P. Fatouros, and F. M. Gasparini, *Phys. Rev. B* **12**, 892 (1975).

¹³D. T. Sprague, N. Alikacem, P. A. Sheldon, and R. B. Hal-

lock, *J. Low Temp. Phys.* **89**, 605 (1992).

¹⁴E. Krotscheck (private communication).

¹⁵E. Krotscheck, M. Saarela, and J. L. Epstein, *Phys. Rev. Lett.* **61**, 1728 (1988).

¹⁶R. H. Anderson and M. D. Miller, *Phys. Rev. B* **40**, 2109 (1989).

¹⁷D. O. Edwards and W. F. Saam, in *Progress in Low Temperature Physics*, edited by D. F. Brewer (North-Holland, Amsterdam, 1978), Vol. VII A, p. 283.

¹⁸W. A. Draisma, M. E. W. Eggenkamp, P. W. H. Pinske, R. Jochenson, and G. Frossati, *Physica B* **194-196**, 853 (1994).

¹⁹R. B. Hallock, *Can. J. Phys.* **65**, 1517 (1987).

²⁰R. M. Heinrichs and R. B. Hallock, in *Helium-75*, edited by I. G. Armitage (World Scientific, Singapore, 1983), p. 40; R. M. Heinrichs, Ph.D. thesis, University of Massachusetts, 1985.

²¹P. A. Sheldon, D. T. Sprague, N. Alikacem, J. Vithayathil, and R. B. Hallock, *Physica B* **194-196**, 877 (1994).

²²F. M. Ellis, J. S. Brooks, and R. B. Hallock, *J. Low Temp. Phys.* **56**, 69 (1984).

²³R. H. Anderson and M. D. Miller, *Phys. Rev. B* **48**, 10426 (1993).

²⁴N. Pavloff and J. Treiner, *J. Low Temp. Phys.* **83**, 15 (1991).